Bulletin of the Seismological Society of America, Vol. 68, No. 2, pp. 429–440, April, 1978

ELSINORE FAULT SEISMICITY: THE SEPTEMBER 13, 1973, AGUA CALIENTE SPRINGS, CALIFORNIA, EARTHQUAKE SERIES

BY M. LEE ALLISON, JAMES H. WHITCOMB, CRAIG E. CHEATUM, AND ROBERT B. MCEUEN

ABSTRACT

A relatively small M_L = 4.8 earthquake and its aftershock series on the southern portion of the Elsinore Fault Zone in eastern San Diego County, California, provided a rare opportunity to study an area that has been subjected to variable tectonic interpretations in the past. Within 12 to 26 hours after the main shock, a network of four portable seismograph stations was established around the main event near Agua Caliente Springs to supplement the stations of the Southern California Seismographic Network. Four days after the main shock, seven additional portable seismograph stations were installed. In addition to the main event, 45 subsequent events were studied, ranging in magnitude from about 1.0 to 3.7. Of these, 36 could be termed aftershocks by their close proximity to the main event, whose proper location was determined by analysis of the aftershock series. Of the two branches of the Elsinore Fault in this region, the south branch is associated with the earthquake series. Focal mechanisms are consistent with right-lateral strike-slip along the south branch, with northeast dip at latitude 32°51'N. These conclusions are supported by hypocentral locations. Thrust activity on the two fault branches may be developing a horst between them, accounting for elevation and tilt changes observed near Agua Caliente.

INTRODUCTION

On September 13, 1973, a M_L = 4.8 earthquake occurred along the Elsinore Fault in the vicinity of Agua Caliente Springs, in eastern San Diego County, California (see Figure 1). The low seismicity of the southern part of the Elsinore Fault makes this event and its aftershock series a rare opportunity to study an area that has been subjected to variable tectonic interpretations. The Elsinore Fault can be traced for more than 200 km from northern Mexico into the Los Angeles basin where it may continue another 32 km as the Whittier Fault (Lamar, 1961). About 32 km of right-slip can be demonstrated on the north half of the Whittier-Elsinore system (Sage, 1973; Lamar, 1961). Yet in the Vallecito Valley area along the southern part of the Elsinore Fault right-slip is 4.8 km or less (Sharp, 1968).

The Elsinore Fault is generally linear over most of its length. The logical projection of it would be southeast through the Tierra Blanca Mountains south of Agua Caliente Springs as seen in Figure 2. However, most maps show it either curving sharply east then sharply south around the mountains through Vallecito and Carrizo valleys or forming a series of subparallel discontinuous breaks in the northeast area of the mountains. In either of these configurations the surface trace of the fault is in an anomalous position northeast of where it might logically be expected. Buttram (1962) mapped a more linear southern branch of the fault across crystalline rock in the Tierra Blanca Mountains but not through an intervening alluviated area known as the Inner Pasture. Weber (1963) carried the fault through the Inner Pasture and does not include on his map the northern (usually considered the main) branch of the fault. He did show a shorter branch passing through Agua Caliente Springs. Buttram (1962) noted the fairly recent scarp on the southern branch (?) in Vallecito Valley. Recent detailed mapping by Todd and Hoggatt

(1976) shows no single through-going fault exposed in Inner Pasture but rather a zone of short faults and gouge planes. They also conclude that movement along this part of the Elsinore Fault has been predominantly vertical. The September 1973 aftershock series centered in the Inner Pasture area near Canebrake Canyon. The present study of the main shock and its aftershock series must therefore try to answer a great many questions. The main objective has been to accurately determine the location of the main or most active branches of the Elsinore Fault and attempt to understand the source mechanism of the main shock and aftershocks, and the tectonic environments of the faults.

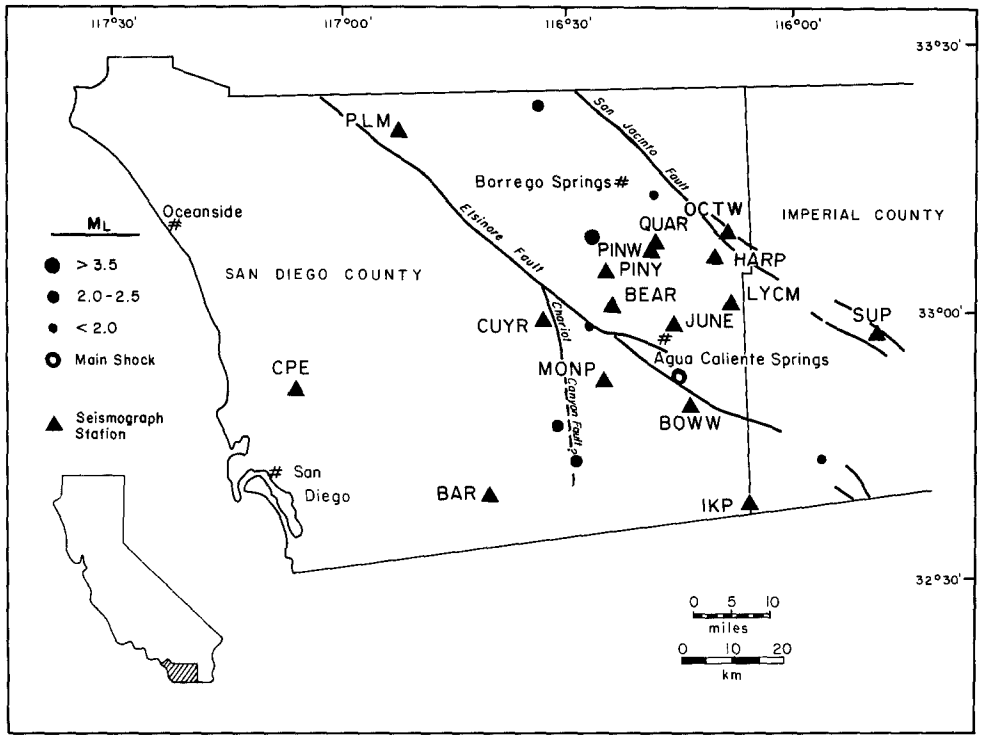

FIG. 1. Location map of San Diego County showing all seismograph stations (triangles) used in epicentral locations and events located outside the aftershock area (circles).

SEISMOLOGICAL ENVIRONMENT

Moderate seismic activity has characterized the southern part of the Elsinore Fault with frequent small events around Agua Caliente Springs, the most active area. No major earthquakes (a M_L = 6.0 or greater) have been reported for this area (Allen *et al.*, 1965). In fact, events greater than M_L = 4.0 are rare (McEuen and Pinckney, 1972).

Previously, the largest earthquake anywhere on the Elsinore Fault in San Diego County was a M_L = 4.5 event in 1969 located approximately in the aftershock area discussed here (San Diego County Comprehensive Planning Organization, 1973). An 1856 earthquake with an intensity of VII was tentatively located south of Banner between the Elsinore and Chariot Canyon Fault. No estimated magnitude for this event has been made. Thus, the earthquake of September 13, 1973, is the largest recorded event related to the Elsinore Fault in San Diego County.

Most seismic activity in San Diego County is associated with the San Jacinto

Fault to the northeast of the Elsinore Fault. An earthquake of $M_L = 6.5$ on the San Jacinto Fault near Borrego Mountain on April 9, 1968, generated wide zones of aftershocks. One cluster of these events covered 10 km, laterally extending northeast from the northern branch of the Elsinore Fault in the area where it bends south to Carrizo Valley, to a point midway between the Elsinore and Coyote Creek Fault (Hamilton, 1972). One aftershock is located on the projected trace of the southern branch of the Elsinore Fault. However, in cross section (southwest to northeast) it is readily apparent that the foci of the events range from about 12-km depth beneath the surface position of the Elsinore Fault upward to 1-km depth to the northeast (Hamilton, 1972). Hamilton suggested that dislocation of the San Jacinto

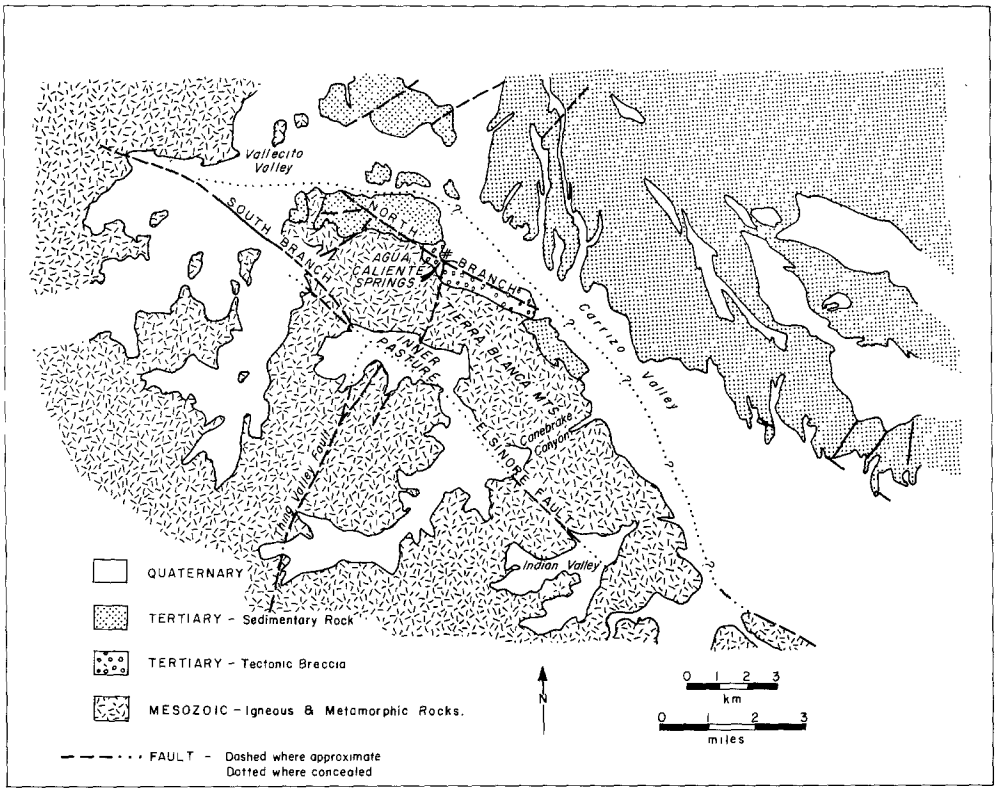

FIG. 2. Generalized geologic map of the Agua Caliente Springs region, San Diego County, California, after Buttram (1962).

Fault by the Borrego Mountain earthquake created zones of stress on either side of the fault that were relieved by aftershocks in the Vallecito Mountain area. Buttram (1962) mapped a number of east-west to northeast-trending faults in this area and described left-lateral offsets on them. A nodal plane solution on one well-determined Borrego Mountain aftershock in this area supports a left-lateral motion on a northeast-trending fault.

A microearthquake study conducted along the entire length of the Elsinore Fault from the Los Angeles basin to the Mexican border showed that most activity is centered in the Vallecito Mountains area (Langenkamp and Combs, 1974). An increase of activity from north to south with 0.5 events per day in the north and 3.7 events per day in the south was noted. Langenkamp and Combs also concluded that the events were mostly less than 5 km deep extending to 12 km in the Agua Caliente Springs area. Their computer program uses an iterative method with 5

km as a starting depth. This study, which uses the same program, investigates the effect of using different starting depths and does not arrive at a markedly different depth distribution.

A composite focal mechanism solution for all events recorded on the Elsinore Fault shows a complicated pattern with no distinct fault plane apparent (Langenkamp and Combs, 1974). Since this covers a 200-km (125 miles) length of the fault, it is unrealistic to expect anything else on such a complicated fault system. In fact, many of the shocks may be related to other faults such as the ones in the Vallecito Mountains.

Data Acquisition

Within 12 to 26 hours after the main shock a network of four portable seismograph stations was established in an array around the main event by the Seismological Laboratory of the California Institute of Technology (Caltech). One trailer was originally placed at Bow Willow then moved to Vallecito Creek after 12 hours of operation. At Vallecito Creek, it ceased to function. Two stations in the mountains, one at Cuyamaca Reservoir and one at Monument Peak, operated from the night of September 13 until battery failure on September 19, 1973. The longest record was made at Ocotillo Wells, lasting until September 20. Positions of the stations are shown in Figure 1. Accurate locations for these stations and the five permanent stations used are summarized in Table 1.

The Agua Caliente Springs area was visited on September 15, 1973, to assess the geological and surficial effects of the earthquake. Residents felt the shock but reported no damage. Many people heard a loud boom from the west (toward the epicenter). Owners of the Crawford Ranch, which is in the center of the aftershock area, were not present during the main event, but could find nothing disturbed in the house.

Park rangers at Agua Caliente Springs reported a slight increase in flow from the springs and stated that this commonly occurred following tremors in this area.

By September 17, 1973, a separate array of seven portable seismograph stations was established north of the aftershock area by the University of California at Riverside (UCR). These stations operated until September 23, and were established to monitor any possible events on the northeast-trending left-lateral faults in the Vallecito Mountains. A total of 21 events were recorded in the vicinity of the aftershock area. All the events were outside the UCR network (by approximately 10 km) and due to the questionable accuracy of their locations are not presented in this paper. However, four of the last five events detected by the Caltech network were also noted on the UCR network. The fifth event was on the order of 100 km north of the main aftershock area. These four events were relocated using the additional stations and the differences between the two sets of locations are minor. The location latitude changes varied from 0.05 to 0.81 min and the location longitudes from 0 to 0.48 min. This agreement with the original locations results in increased confidence in the location of the remainder of the Caltech determined events.

Hypocentral Locations

All shocks that could be accurately located (recorded at three or more stations) are listed in Table 2. Thirty-six aftershocks ranging in magnitude from about 1.0 to 3.65 are shown in Figure 3. Of an additional nine events recorded, seven are within the limits of the index map (Figure 1) and two are outside. This listing is considered complete as the record of each station was searched independently,

then researched, looking for additional events from a master compilation.

Travel-time corrections are based in all but one case solely on the elevation of the station. A P-wave velocity of 5.1 km/sec was used in calculations of elevation corrections. Bow Willow has a geological correction of +0.1 sec to compensate for thick alluvium. The correction factors thus obtained are summarized in Table 1.

All of the travel-time correction factors were applied to a five-layer southern California crustal model from Gutenberg (1955), used in the computer location program. In actuality, this model is a gross simplification, local geology and crustal structure being complicated and variable. However, these local variations average out regionally to a good approximation of the Gutenberg model as evidenced by the quality of the epicenter locations.

The hypocentral locations were determined using both P and S arrivals. The

TABLE 1

SEISMOGRAPHIC STATIONS USED IN EPICENTRAL LOCATIONS: CIT, CALIFORNIA INSTITUTE OF TECHNOLOGY AND UCR, UNIVERSITY OF CALIFORNIA, RIVERSIDE

	Station	Lat. N	Long. W	Elev. (meters)	Delay (sec)	Distance* (km)	Period of Operation	Operator
BAR	Barrett	32 40.80	116 40.30	510	0.07	45.2	Permanent	CIT
BEAR	Blair Valley	33 00.76	116 23.45	841	0.12	18.4	9/17-9/23	UCR
BOWW	Bow Willow	32 50.57	116 13.68	325	0.15	6.2	9/14	CIT
CPE	Camp Elliott	32 52.80	117 06.00	213	0.03	75.9	Permanent	CIT
CUYR	Cuyamaca Reservoir	33 00.30	116 33.38	1475	0.20	30.2	9/13-9/16	CIT
HARP	Harper Canyon	33 06.67	116 10.13	140	0.04	25.9	9/17-9/23	UCR
IKP	In-Ko-Pah	32 38.93	116 06.48	957	0.13	30.5	Permanent	CIT
JUNE	June Wash	32 57.94	116 15.47	427	0.26	8.3	9/17-9/23	UCR
LYCM	Lycium Wash	33 01.05	116 07.96	207	0.23	18.4	9/17-9/23	UCR
MONP	Monument Peak	32 53.42	116 25.53	1850	0.26	13.0	9/14-9/16	CIT
OCTW	Ocotillo Wells	33 09.60	116 09.04	88	0.01	30.3	9/13-9/20	CIT
PINW	Pinyon Wash	33 06.73	116 18.54	463	0.07	25.1	9/17-9/23	UCR
PINY	Pinyon Mtns	33 04.02	116 24.49	774	0.11	22.1	9/17-9/23	UCR
PLM	Palomar	33 21.20	116 51.70	1692	0.23	74.0	Permanent	CIT
QUAR	Quartz Vein Wash	33 07.64	116 17.73	266	0.04	26.6	9/17-9/23	UCR
SUP	Superstition Mountain	32 57.31	115 49.42	226	0.03	41.4	Permanent	CIT

* Distance to main shock location 32 53.50N, 116 15.50W.

locations were also determined using P waves only because of uncertainty associated with reading S arrivals. There is no significant difference in the distribution or location of the aftershocks between the two determinations.

Hypocenters of the aftershocks were determined using HYP071, a computer program written by Lee and Lahr (1971). The station nearest the earthquake is chosen as a trial epicenter and adjustments are made to this trial location in a series of iterations until the root-mean-square (RMS) error in the travel times to the various stations is less than 0.5 sec. For the 36 aftershocks the RMS error varied from 0.08 to 0.48 sec. This implies an apparent epicentral location error of 0.4 to 2.5 km. One problem encountered was the tendency to converge on depths near the arbitrary trial starting depths. In order to get a better understanding of the depths, the hypocenters were computed using three different initial trial depths: 2, 8, and 20 km. Most of the 2-km hypocenters remained at 2 km while the 8-km trial hypocenters were changed in both directions and the 20-km hypocenters were usually made shallower. These variations give some estimate of the constraints

TABLE 2

DEPTHS OF EVENTS CALCULATED FROM HYP071 USING DIFFERENT TPIAL DEPTHS

Events (Date)	Time (GMT)	Trial Depths (km)*		
		2	8	20
9–13	1738	2.00	8.00	20.00
	1740	2.00	8.00	16.75
	1815	2.00	9.54	11.82
	1826	2.00	2.44	14.18
	1842	2.00	3.44	2.75
	1850	2.00	12.25	21.27
	1859	2.00	8.00	17.88
	1958	2.00	2.78	15.66
	2110	2.00	8.00	20.00
	2210	2.00	2.26	20.00
	2230	2.00	4.18	2.38
	2248	2.00	8.00	12.77
	2255	2.00	6.18	20.00
	2347	2.00	8.00	20.00
9–14	0027	2.00	5.44	10.30
	0235	2.00	8.00	16.28
	0312	2.00	7.44	14.53
	0524	2.00	6.31	9.20
	0556	2.00	8.00	12.30
	0558	2.00	8.00	12.85
	0607	2.00	8.97	12.13
	0704	2.00	8.00	9.49
	0907	2.00	7.31	5.92
	1005	2.00	13.99	14.06
	1038	2.00	11.47	12.73
	1058	2.00	8.00	9.44
	2322	2.00	4.59	12.75
9–15	0045	2.00	8.00	8.75
	0253	2.00	8.00	8.61
	0515	2.00	8.00	12.69
	0527	2.00	8.00	13.25
	0611	2.00	8.00	11.71
	1505	9.61	9.60	9.64
	1854	2.00	2.06	11.90
	1947	2.00	8.00	12.94
	2000	2.00	8.00	13.40
	2236	2.00	3.79	12.31
9–16	0722	2.00	3.28	4.40
	1339	2.00	3.18	6.42
	1504	2.00	8.00	8.08
9–18	1528	2.00	4.53	10.85
9–19	0001	2.00	8.00	10.14
	1142	9.80	9.52	13.31
9–20	0110	2.00	8.00	8.98
9–21	1646	2.00	8.00	14.09

* Hypocentral depths computed from trial depths.

that initial assumptions impose on the depths for a fixed velocity model. The depths have been summarized in Table 2 and projected onto cross section shown in Figure 4.

Hypocenters obtained in this study have been divided into three categories of

accuracy (Table 3), depending on the standard error of the computer solution. "A" quality locations are believed to be accurate to within 2 km horizontally and 4 km vertically; "B" quality hypocenters to within 4 km horizontally and 8 km vertically; and "C" quality locations are less accurate. The quality is determined by comparing

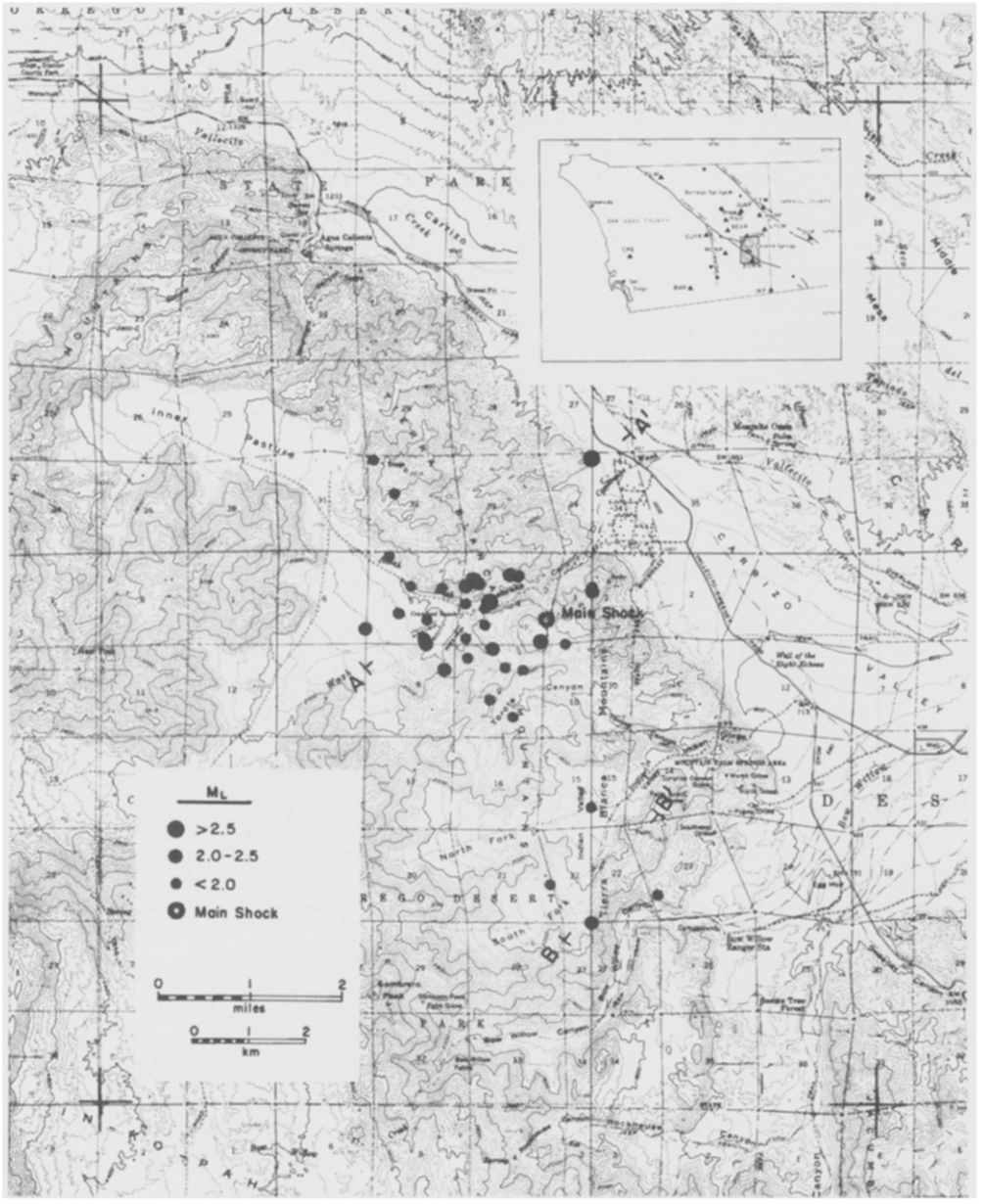

FIG. 3. Epicenters of the Agua Caliente Springs aftershocks for September 13–20, 1973.

the horizontal quality to the vertical quality such as (A, C) = B or (C, C) = C. In a case such as (B, C), the lower value C is taken as the quality.

The first hypocentral locations are poorer than those for events after the portable stations were installed because of the distance of the aftershock area from the permanent stations of the Southern California seismic network. The depth of the

main shock is not known. However, preliminary location of the main shock, originally determined to be 32°57.15N and 116°16.77W can be improved by comparing relative arrival times at the permanent stations between the main shock and the aftershocks. Relative times for the main shock are essentially the same as those for the much more accurately located aftershock series. This means the main shock should be at the same location as the aftershocks, about 6 km south of its original location. More precise relative location methods were not attempted because of inconsistencies in aftershock data as recorded at distant stations. Thus, the epicenter of the main shock is placed at 32°53.50N; 116°15.50W near the center of the aftershocks on the southern branch of the Elsinore Fault.

An apparent migration of aftershock activity inward toward the center of the

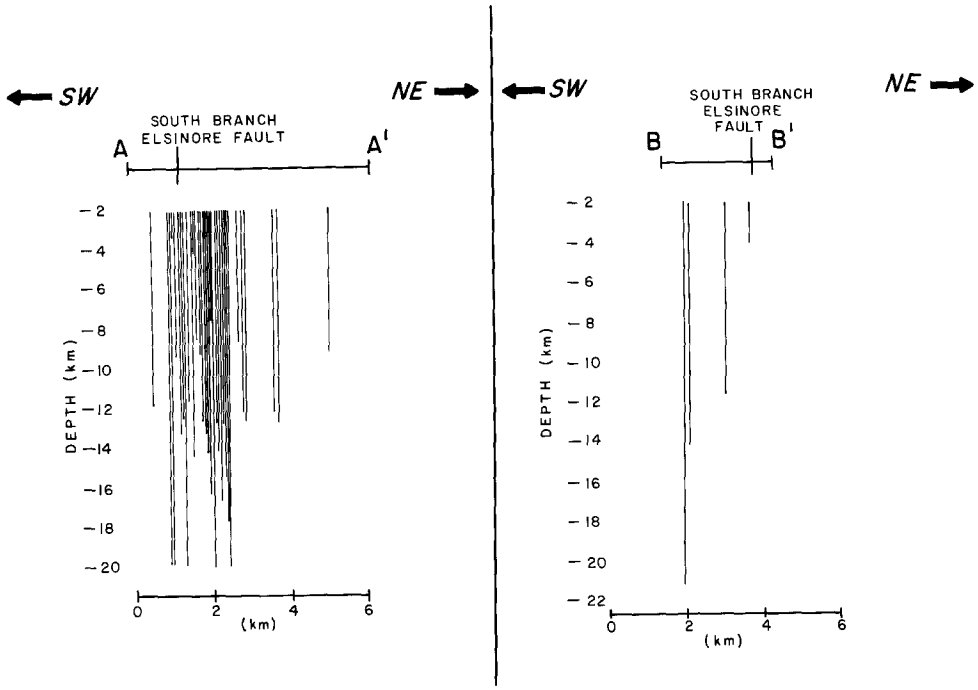

FIG. 4. Cross-sections showing range of depths of aftershocks calculated from HYPO71 using different trial depths. Aftershock locations are projected onto the cross-sections shown in Figure 3. (A-A') Inner Pasture-Canebrake Canyon; (B-B') Indian Valley.

aftershock area after the first 24 hr is most likely the result of more accurate locations from the portable stations joining the network. The shocks decreased in number during the week they were analyzed. From September 15 until the end of the study period on September 21, the majority of the events recorded were outside the aftershock area. Two of the events occurred along the recently discovered Chariot Canyon Fault near Buckman Springs (Allison, 1974).

MAGNITUDES

A magnitude of M_L = 4.8 was assigned by Caltech for the Agua Caliente main shock. Magnitudes have been assigned to aftershocks (Table 3) on the basis of readings from the closest standard Wood-Anderson torsion seismometer at Barrett (BAR). In general, they compare well with the few magnitudes of the smaller

TABLE 3

AFTERSHOCKS OF THE AGUA CALIENTE EARTHQUAKE AND OTHER LOCATED EVENTS FROM SEPTEMBER 13 TO SEPTEMBER 21, 1973

Date	Time	(GCT)	Lat. N.	Long. W.	Depth (km)	Q*	Magnitude†	
							M_L	M (CIT)
Main Shock	1730	39.76	32 53.50	116 15.50				4.8
9–13	1738	01.50	32 53.02	116 16.65	2.–20.00	C	2.3	
	1740	00.88	32 53.65	116 16.14	2.–16.75	B	2.7	2.3
	1815	52.78	32 50.90	116 14.26	2.–11.82	C		
	1826	26.56	32 53.80	116 16.41	2.–14.18	B	2.4	
	1842	14.86	32 53.55	116 17.17	2.–3.44	A		
	1850	52.98	32 50.63	116 15.00	2.–21.27	C	2.2	
	1859	03.29	32 53.84	116 16.27	2.–17.88	B	2.2	
	1958	45.61	32 54.68	116 17.21	2.–15.66	C	1.9	
	2110	50.62	32 53.26	116 16.86	2.–20.00	B	2.2	
	2210	36.63	32 55.00	116 17.44	2.–20.00	C		
	2230	19.94	32 54.09	116 17.27	2.–4.18	A	1.9	
	2248	44.99	32 53.85	116 16.33	2.–12.77	B	3.1	3.2
	2255	44.77	32 53.48	116 16.85	2.–20.00	B	1.9	
	2347	33.71	32 53.44	116 16.20	2.–20.00	B	1.9	
9–14	0028	01.46	32 44.12	116 29.36	2.–10.30	C	2.3	2.7
	0235	03.13	32 53.02	116 15.77	2.–16.28	C	1.9	
	0312	49.20	32 53.80	116 17.02	2.–14.53	B		
	0524	24.68	32 55.00	116 15.00	2.–9.20	B	3.1	3.0
	0556	50.13	32 53.91	116 15.92	2.–12.30	B	3.0	2.8
	0558	06.60	32 53.21	116 16.11	2.–12.85	B	2.6	
	0607	15.37	32 53.76	116 15.00	2.–12.13	B	2.3	
	0704	42.17	32 53.30	116 16.87	2.–9.49	B	2.5	2.9
	0907	43.95	32 53.64	116 16.42	2.–7.31	B	1.9	
	1005	26.20	32 51.00	116 15.45	2.–14.06	B	1.9	
	1038	20.11	32 52.57	116 15.88	2.–12.73	B		
	1058	02.67	32 53.04	116 15.97	2.–9.44	B	1.9	
	2322	37.49	32 53.79	116 15.00	2.–12.75	B		
9–15	0045	21.15	32 53.26	116 15.30	2.–8.75	B		
	0253	41.32	32 53.31	116 16.41	2.–8.61	B	1.9	
	0515	50.61	32 53.61	116 16.20	2.–12.69	B		
	0527	05.66	32 53.79	116 16.68	2.–13.25	B		
	0611	29.54	32 53.39	116 17.54	2.–11.71	B	2.2	
	1505	26.64	33 24.46	116 33.68	9.60–9.64	A	2.3	2.3
	1854	35.42	32 53.13	116 16.39	2.–11.90	B		
	1947	58.01	32 53.90	116 15.83	2.–12.94	B		
	2000	10.83	32 52.74	116 16.14	2.–13.40	B		
	2236	05.49	32 13.26	115 46.44	2.–12.31	B		
9–16	0722	01.53	32 51.73	116 15.00	2.–4.40	B		
	1339	53.73	33 14.38	116 18.39	2.–6.42	B		
	1504	11.59	32 43.76	115 57.08	2.–8.08	C		
9–18	1528	22.69	32 59.49	116 27.56	2.–10.85	B		
9–19	0001	00.08	33 10.27	116 26.40	2.–10.14	B	3.55	3.4
	1141	57.44	33 41.29	116 45.07	2.–13.31	C	2.75	2.3
9–20	0110	18.83	32 48.63	116 31.61	2.–8.98	B	2.1	2.5
9–21	1646	27.80	32 53.30	116 15.57	2.–14.09	C	2.5	

* An explanation of quality (Q) is given in the text.

† Magnitudes assigned in this study are labeled M_L, while magnitudes assigned by Caltech are labeled M(CIT). Blanks in the M_L column indicate magnitudes less than 1.9; in the M(CIT) column, indicate magnitudes not assigned.

aftershocks assigned by Caltech. Discrepancies are generally within the 0.30 average standard deviation found by Allen *et al.* (1975) for the San Fernando aftershock series using Caltech data.

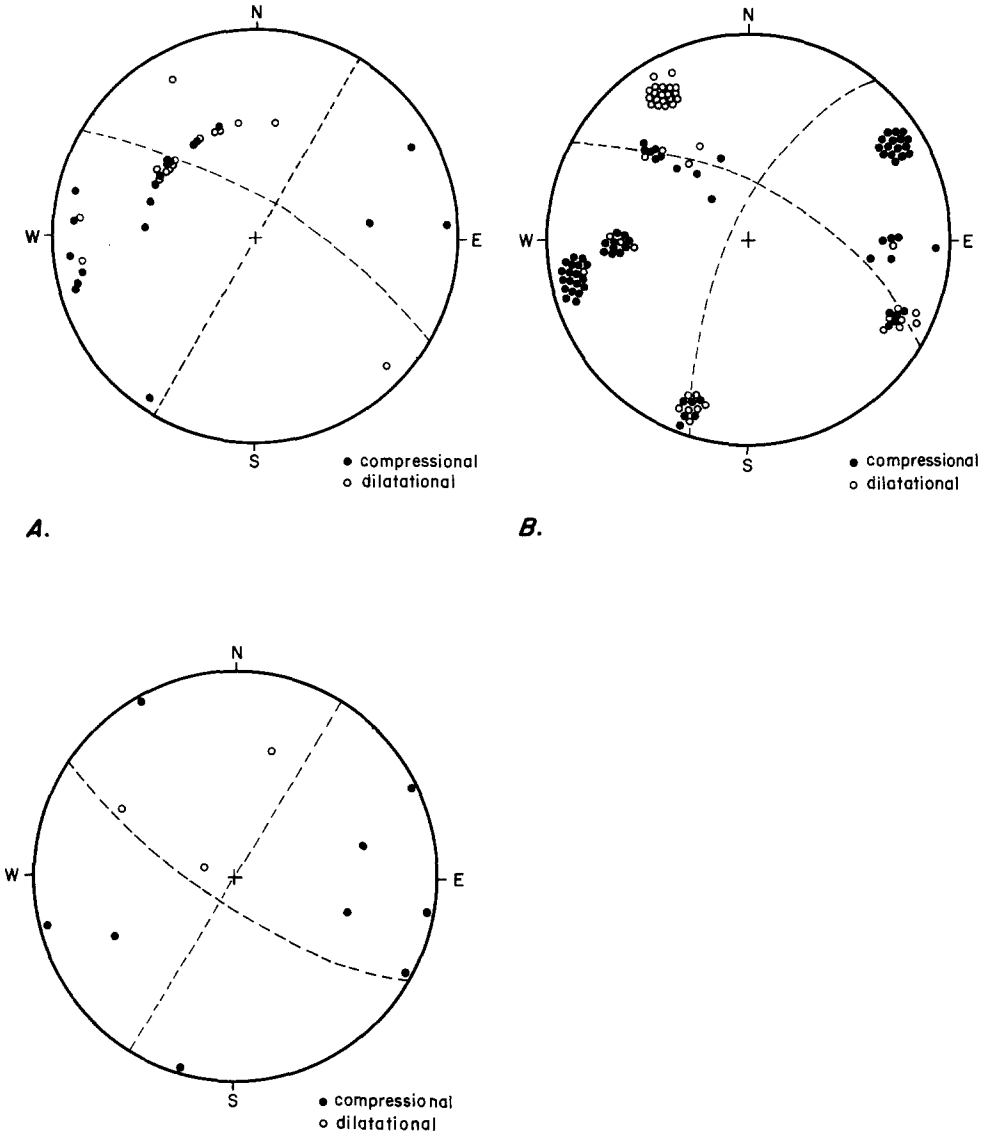

FIG. 5. Composite fault-plane solutions. (A) Main shock, from 38 stations in southern California, the nodal plane trends N60°W; (B) Inner Pasture-Canebrake Canyon aftershocks; the nodal plane trends N60°W; (C) Indian Valley aftershocks, the nodal plane trends N58°W. Lower hemisphere equal-area projections.

FOCAL MECHANISMS

Focal mechanism solutions for the main shock and for all aftershocks that were recorded at five or more stations are presented in Figure 5. Although the total number of events that can be analyzed this way is relatively small (31 events), it appears adequate to interpret the results.

The basic mechanism of initial faulting was that of a right-lateral strike-slip fault striking about N60°W, dipping steeply to the northeast, and including a minor component of thrusting to the northwest. Subsequent stress release was also of right-lateral slip presumably along the south branch of the Elsinore Fault.

Most of the aftershocks, which began immediately after the main shock, indicate a steeply northeast-dipping fault plane along the southern branch of the Elsinore Fault. A group of four hypocentral locations southeast of the main area in the Indian Valley area strongly define a steep southwest-dipping fault plane. Three of the four events occurred during the first 24 hr of the aftershock series.

A composite first-motion plot has been compiled of all aftershocks in the Inner Pasture-Canebrake Canyon area except for one suggesting thrusting. This composite tends to support a northwest-trending fault with right-lateral slip and a minor component of northwest thrusting. The composite suggests a fault trend of N60°W and the dip is probably steep and to the northeast. First-motion plots of the four events to the southeast in Indian Valley also suggest right-lateral slip but with less of a thrust component. The fault plane is northwest-trending (N58°W) but with a more near-vertical or southwesterly dip than that of the main cluster of aftershocks.

It is clear that the focal mechanism of the main shock is not well determined but it is consistent with the composite focal mechanism. Neither is well constrained, but if one were to impose a condition that the rupture have the same approximate strike as the south branch of the Elsinore Fault, the composite and main shock focal mechanisms are well constrained. The mapped trend of the fault is about N50°W, which is close to the values obtained for the focal mechanisms. The two focal mechanisms give a steep northeast dip which is consistent with the epicenter distribution to the northeast of the fault.

Discussion

The series of small discontinuous faults mapped by Todd and Hoggatt (1976) may explain the poor constraints on the composite focal mechanism solutions. The composite solutions may represent strain release on a number of small faults of slightly different orientation and dip. Hypocentral locations and focal mechanisms probably show general trends of the fault zones rather than exact placement and orientation of particular fault planes.

Buttram (1962) believes that uplift and tilting is occurring in the area around Agua Caliente Springs. Additionally, along the trace of the south branch of the Elsinore Fault in the Inner Pasture he mapped a unit of older alluvium that is higher than younger alluvium to the south and is being eroded.

Buttram (1962) also mapped a few small faults in the north part of the Tierra Blanca Mountains which show relative uplift of the mountain block. Evidence presented here suggests that this mountain block, which is essentially defined by the southern branch of the Elsinore Fault and the discontinuous breaks to the northeast, is being elevated and tilted by thrust action along these predominantly strike-slip faults.

Thus, the following conclusions are made:

1. The south branch of the Elsinore Fault is active;
2. the focal mechanisms are consistent with right-lateral strike-slip along the south branch with northeast dip in the main area and southwest dip in the southerly area;
3. hypocentral locations support conclusion (2);
4. the aftershocks migrated toward the center of the aftershock area during the first 24 hr after the main event; and

5. there is a component of thrusting on the fault branches which needs to be further studied in relation to elevation and tilt changes in the Tierra Blanca Mountains near Agua Caliente.

ACKNOWLEDGMENTS

The authors thank the Caltech personnel who helped to organize and perform the field installations. This work was partially supported by the Caltech Earthquake Research Affiliates and by grants from the U. S. Geological Survey, the Jet Propulsion Laboratory, and the University of California, Riverside Intramural Fund. We also thank Standard Oil Company of California for help in preparation of this manuscript and illustrations. Ellen McLean critically reviewed the paper and provided many helpful suggestions.

REFERENCES

Allen, C. R., P. St. Amand, C. F. Richter, and J. M. Nordquist (1965). Relationship between seismicity and geologic structure in the southern California region, *Bull. Seism. Soc. Am.* **55,** 753–797.

Allen, C. R., T. C. Hanks, and J. H. Whitcomb (1975). Seismological studies of the San Fernando earthquake and their tectonic implications, in San Fernando, California, Earthquake of 9 February, 1971, G. B. Oakeshott, Editor, *Calif. Div. Mines Geol. Bull.* **196,** 257–262.

Allison, M. L. (1974). Tectonic relationship of the Elsinore Fault Zone and the Chariot Canyon Fault, San Diego County, California (abstract), Abstracts with Programs, *Bull. Geol. Soc. Am.* **6,** 138.

Buttram, G. N. (1962). Geology of the Agua Caliente Springs quadrangle (California) (M. S. thesis) Univ. of Southern California, Los Angeles, 96 pp.

Comprehensive Planning Organization (1973). Open space study—phase II and model seismic safety element, San Diego County, California, earthquake and fault map.

Gutenberg, B. (1955). Wave velocities in the earth's crust, Geol. Soc. Am. Special Paper 62, 19–34.

Hamilton, R. M. (1972). Aftershocks of the Borrego Mountain earthquake from April 9, 1968, U. S. Geol. Surv. Profess. Paper 787, 31–55.

Lamar, D. L. (1961). Structural evolution of the northern margin of the Los Angeles basin, unpub. Ph.D. thesis, Univ. California, Los Angeles, 142 pp.

Langenkamp, D. and J. Combs (1974). Microearthquake study of the Elsinore fault zone, southern California, Bull. Seism. Soc. Am. **68,** 187–203.

Lee, W. H. K. and J. C. Lahr (1971). HYPO71, a computer program for determining hypocenter, magnitude, and first motion pattern of local earthquakes, U. S. Geol. Surv. Open File Rept. 112 pp.

McEuen, R. B. and C. J. Pinckney (1972). Seismic risk in San Diego, Trans. San Diego Soc. Nat. Hist. **17,** 33–62.

Sage, O. G., Jr. (1973). Paleocene geography of the Los Angeles region, in *Proc. Conf. Tectonic Problems San Andreas Fault System,* Stanford Univ. Pub., Geol. Sci. **XIII,** 348–357.

Sharp, R. V. (1968). The San Andreas fault system and contrasting pre-San Andreas structure in the Peninsular Ranges of southern California, in *Proc. Conf. Geol. Problems San Andreas Fault System,* W. R. Dickinson and A. Grantz, Editors, Stanford Univ. Pub. Sci., **XI,** 292–293.

Todd, V. R. and W. C. Hoggatt (1976). The Elsinore Fault Zone in the Tierra Blanca Mountains, Eastern San Diego County, California (abstract), Abstracts with Programs, *Bull. Geol. Soc. Am.* **8,** 416.

Weber, H. F. Jr. (1963). Geology and mineral resources of San Diego County, California, *Calif. Div. Mines Geol. County Rept.* **3,** 309 pp.

STANDARD OIL COMPANY OF CALIFORNIA
575 MARKET STREET
SAN FRANCISCO, CALIFORNIA 94105 (M.L.A.)

HARDING-LAWSON ASSOCIATES
HOUSTON, TEXAS 77036 (C.E.C.)

Manuscript received August 12, 1977

SEISMOLOGICAL LABORATORY
CALIFORNIA INSTITUTE OF TECHNOLOGY
PASADENA, CALIFORNIA 91125 (J.H.W.)

CONTRIBUTION NO. 2881

DEPARTMENT OF GEOLOGICAL SCIENCES
SAN DIEGO STATE UNIVERSITY
SAN DIEGO, CALIFORNIA 92182 (R.B.MCE.)